Case Studies in Chemical and Environmental Engineering 8 (2023) 100405

Contents lists available at ScienceDirect

Case Studies in Chemical and Environmental Engineering

journal homepage: www.sciencedirect.com/journal/case-studies-in-chemical-and-environmental-engineering

Case Report

Investigation of effective parameters in the production of alumina gel through the sol-gel method

Rusul Alabada [a], Mustafa M. Kadhim [b], Zainab sabri Abbas [c], Ahmed Mahdi Rheima [d], Usama S. Altimari [e], Ashour H. Dawood [f], Alaa dhari jawad al-bayati [g], Zainab Talib Abed [h], Rusul Saeed Radhi [i], Asala Salam Jaber [j], Safa K. Hachim [k,l], Farah K. Ali [m], Zaid H. Mahmoud [n], Ehsan Kianfar [o,p,q,*]

[a] *Al-Muthanna University, College of Nursing, Iraq*
[b] *Medical Laboratory Techniques Department, Al-Farahidi University, Baghdad, 10022, Iraq*
[c] *Wasit university, college of science, department of chemistry, Iraq*
[d] *Department of Chemistry, College of Science, Mustansiriyah University, Baghdad, Iraq*
[e] *Department of Medical Laboratories Technology, AL-Nisour University College, Baghdad, Iraq*
[f] *department of medical engineering/ Al-Esraa University College, Baghdad, Iraq*
[g] *Department of chemical Engineering and petroleum Industries, Al-Mustaqbal University College, Hilla, 51001, Iraq*
[h] *College of Pharmacy, The University of Mashreq, 10021, Baghdad, Iraq*
[i] *Wasit university, college of science, department of physics, Iraq*
[j] *Department of pharmacy, Mazaya university college, Thi-Qar, Iraq*
[k] *College of technical engineering, The Islamic University, Najaf, Iraq*
[l] *Department of Medical Laboratory, College of Health and Medical Technology, National University of Science and Technology, Thi-Qar, 64001, Iraq*
[m] *Medical Laboratory Techniques Department, Al-Turath University College, Baghdad, Iraq*
[n] *University of Diyala, college of sciences, chemistry, Diyala, Iraq*
[o] *Mechanical Engineering Department, Faculty of Engineering and Pure Sciences, Istanbul Medeniyet University, Istanbul, Turkey*
[p] *Department of Chemical Engineering, Arak Branch, Islamic Azad University, Arak, Iran*
[q] *Young Researchers and Elite Club, Garcharan Branch, Islamic Azad University, Gachsaran, Iran*

ARTICLE INFO

Keywords:
Alumina gel
Effective parameters
Gelation point
Supercritical
CO_2
Aerogel

ABSTRACT

Sol-gel chemistry is currently applied as one of the most widely used methods for synthesis of nanoparticles. In this method hydrolysis and poly-condensation reactions occur when the gel precursors are mixed with water and catalyst. The further condensation of sol particles into a three-dimensional network produces a gel. There are several parameters that effect on gelation time such as the molar ratio of alkoxide to water, the rate of hydrolysis, the type and amount of catalyst used, initial concentration of precursors and the temperature of hydrolysis and drying. Encapsulated solvent can be removed from a gel by either evaporative drying or supercritical drying. Where the resulting solids are known as a xerogel and an aerogel, respectively. During the drying process due to the surface tension of the liquid, a capillary pressure gradient is built in the pore walls, which is able to collapse most part of the pore volume. The volume shrinkage may be prevented by supercritical drying. The strength, thermal stability, pore structure and morphology of aerogels are keys to success for wider applications such as catalyst supports, thermal and acoustic insulators and adsorbents. Among catalyst support materials, alumina became popular recently due to its highly thermal and chemical stability and higher porosity. In the present study, synthesis of alumina gel as a support for nano-catalysts through hydrolysis of aluminum tri-sec-butoxide (ASB) in ethanol was investigated. The gel synthesis was carried out at 32 and 60 °C with different concentrations of water and precursor and different types and amounts of acid as catalyst. Rate of gel formation, efficiency of hydrolysis and polymerization and amount of gel production were measured and discussed. Results showed that acid addition around 0.2 ml and water to ASB malar ratio of 2 at 60 °C maximized the amount of gel produced and minimized the gelation time. Then, the alumina gel that synthesized at optimum conditions was dried by two different methods, at atmospheric pressure and temperature and at supercritical conditions of carbon dioxide and the results of Scanning Electron Microscopy were compared.

* Corresponding author. Mechanical Engineering Department, Faculty of Engineering and Pure Sciences, Istanbul Medeniyet University, Istanbul, Turkey.
E-mail address: ehsan_kianfar2010@yahoo.com (E. Kianfar).

https://doi.org/10.1016/j.cscee.2023.100405
Received 22 May 2023; Received in revised form 13 June 2023; Accepted 17 June 2023
Available online 19 June 2023

1. Introduction

sol-gel is a Wet Chemical Method for the synthesis of various nanostructures, especially metal oxide nanoparticles. In this method, the molecular precursor (usually metal alkoxide) is dissolved in water or alcohol the gel due to hydrolysis/Alkalize with heat and stirring [1–5]. Fig. 1 shows Schematic representation of the different stages and routes of the sol–gel technology.

For the first time in 1845, Ebelman accidently observed that silicon tetrachloride ($SiCl_4$), which was left in a container, first hydrolyzed and then turned into a gel. about a century, the sol-gel method was only of interest to chemists, but in 1930, Schott Company used the sol-gel method to coat industrial glass with oxide layers using metal compounds as precursors [6–10].

Mineral gels from poly aqueous salts have been studied for a long time [8,9]. Graham showed that the water inside the silica gel can be replaced by organic solvents, which confirmed the theory of the porous structure of the solid gel network [11–14]. While other theories considered the structure of the gel as a coagulated sol whose particles are surrounded by a layer of water or an Emulsion. In the 1930s, the network and porous structure of gel was widely accepted, which was the result of hard work [15–20]. The synthesis of Aerogel by drying the gel using supercritical fluid by Kistler in 1932 was also a confirmation of the network structure of the gel [20–25]. At the same time, the production of homogeneous powder from gel and sol for study in the field of phase balance received a lot of attention. It is worth mentioning that with this method, many inorganic oxides such as TiO_2, SiO_2, ZrO_2 were synthesized [26–30]. The main reasons for using the sol-gel are to a product with high purity, to distribute the size of fine particles and to achieve a uniform nanostructure. The sol-gel is often use for the synthesis of metal nano oxides [31–35]. The materials obtained from the sol-gel preparation method can be used in different optical, electronic, energy, surface, biosensors, pharmaceutical and separation technology such as chromatography [36–40].

Yoldas et al. [2], investigated the effect of electrolyte concentration on the volume of alumina gel synthesized during the sol-gel process. She came to the conclusion that when the electrolyte concentration is approximately 0.07 mol per mol of hydroxide, the relative volume of the gel goes to its lowest value [3,41–45].

Walendziewski et al. [4], investigated the effective parameters including the type of precursor and solvent, gel synthesis and drying temperature, and Aerogel calcination temperature on the density, surface area, and total volume of the voids and showed that the highest surface area is related to Aerogel. with aluminum isopropoxide precursor with methanol solvent and the molar ratio of water to precursor equal to 9 at the hydrolysis temperature of 20 °C and the lowest density of the Aerogel was related to the same conditions at the hydrolysis temperature of 60 °C [5].

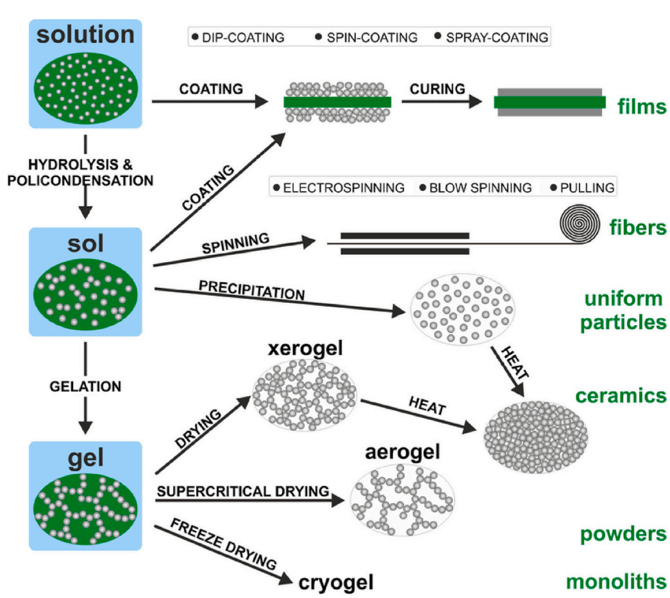

Fig. 1. Schematic representation of the different stages and routes of the sol–gel technology [1].

Poco et al. [6], presented a two-step synthesis method for a monolithic alumina aerogel with a porosity above 98%. They used water with a molar ratio lower than the stoichiometric ratio and acetic acid as the hydrolysis catalyst [46–48]. After changing the solvent, it was dried with the help of supercritical ethanol conditions. The obtained Aerogel was compared with silica Aerogel with the same density [49–52]. Thermal resistance and elastic modulus were higher than silica Aerogel, but the specific area was lower [53–57].

Bihan et al. [7], studied the synthesis of alumina Aerogel and compared the effects of two substances, acetylacetone and butan-1, 3-diol as complexing agents in different proportions, and concluded that the maximum area The specific one related to Aerogel with acetylacetonate complex-forming agent in a molar ratio equal to one to the precursor, and the largest cavity volume is related to Aerogel without complexing agent.

Sharma et al. [8], showed the important role of sol-alumina pH in the morphology and size of alpha-alumina particles in the sol-gel synthesis method and stated that by changing the pH from 12 to 2.5, the size of alumina particles from 750 to 70 nm decrease.

Bono et al. [9], synthesized alumina aerogel using the method presented for the synthesis of alumina gel by Armor and his colleagues in 1987 and with the help of a fast supercritical method, and the effect of nitric acid concentration in alumina sol on the specific area, density and investigated the microstructure of Aerogel. Methanol extraction was done under supercritical conditions in 7.5 h. The results showed that with the increase in the amount of acid, the bulk density decreases and the specific area increases [58–63]. Acid concentration also affects the morphology of Aerogel. This result was contrary to the results obtained in aerogels prepared by other methods, which can indicate the effect of controlled parameters such as time of acid addition, type of solvent and different method of Aerogel synthesis [64–68]. They also stated that uncontrolled environmental factors such as humidity can also be involved in the synthesis and the results obtained [69–73].

Alumina is one of the most important technical ceramics. It has versatile uses, such as lasers, lamp covers, thread guides, catalytic converters and substrates for microelectronic computer chips. Yoldas [1–3] synthesized monoliths of alumina by sol-gel technology in which the sol precursor used was an aluminium alkoxide. Yoldas process consists of four steps: (1) hydrolysis of aluminium alkoxides, (2) peptization of the hydroxide to a sol, (3) gel formation and (4) pyrolysis of the dried gel to alumina [74–80].

Due to their very strongly developed porous structure, large pore volume (even larger than 5 cm^3/g) and high specific surface area [81–84], aerogel materials are very interesting materials and can find many different applications [85–89]. They are mainly obtained by hydrolysis of organic metal compounds, gelation of sol and drying under supercritical conditions the solvent used. Both the hydrolysis and gelation reactions proceed under strictly controlled conditions, which allow to obtain gels of the claimed properties and do not allow aluminium hydroxide to precipitate. Drying of alumina gels under supercritical conditions ensures the porous aerogel structure to be maintained. It was stated in our first paper that the main parameters influencing the pore structure of alumina aerogels are the type of solvent and concentration of aerogel precursor [90–94]. However, the pore structure of alumina aerogels depends also on synthesis conditions, and drying and calcination conditions. In this paper we present data on the influence of synthesis parameters (temperature, type of precursor and solvent), drying and calcination conditions on the textural properties of alumina aerogels that may be applied as catalyst supports [95–100].

The purpose of this article is that the sol-gel method is a suitable and common method for producing alumina. In this method, aluminum alkoxide is dissolved in a suitable solvent, then it is hydrolyzed with water in the presence of an acid as a catalyst. Hydrolysis and polymerization reactions take place and gel is formed. Many parameters, such as the ratio of water and acid to alkoxide, the temperature of hydrolysis and gel formation, the initial concentration of the precursor in the solvent, whether the hydrolysis is one-stage or two-stage, and the method of drying the gel, have an effect on the formation of alumina gel and its final structure. The aim of this research investigates parameters and obtain the largest gel volume in the shortest possible time and synthesize alumina with a porous structure suitable for catalytic applications. Then, the alumina gel that synthesized at optimum conditions was dried by two different methods, at atmospheric pressure and temperature and at supercritical conditions of carbon dioxide and the results of Scanning Electron Microscopy were compared. It is hoped that at the end of this article, a suitable and optimal method for the synthesis of alumina and its use as a catalyst base will be presented.

2. Method and materials

2.1. Magnetic stirrer with heater

A magnetic stirrer with a heater was used to stir the solution for gel synthesis and to simultaneously heat it to a certain temperature.

2.2. Supercritical dryer

In order to dry the gel in supercritical conditions, an existing laboratory device was used. The basis of this device consists of a reactor under pressure with a volume of 250 ml, which is immersed in a paraffin bath to adjust the temperature. Fig. 2 show the schematic view of this laboratory device.

2.3. Reactor

The device uses a reactor with a volume of 250 ml. This reactor includes a gas inlet as well as an outlet. The pressure inside the reactor is sensed by a digital pressure gauge and its temperature by a thermocouple. The reactor is made of 316 stainless steel and can withstand pressure up to 7000 psi.

2.4. Paraffin bath

In order to control the temperature in the drying process of the gel, a bath with the ability to control the temperature in the range of −20 to 100 °C is used. Paraffin fluid is used in this bath.

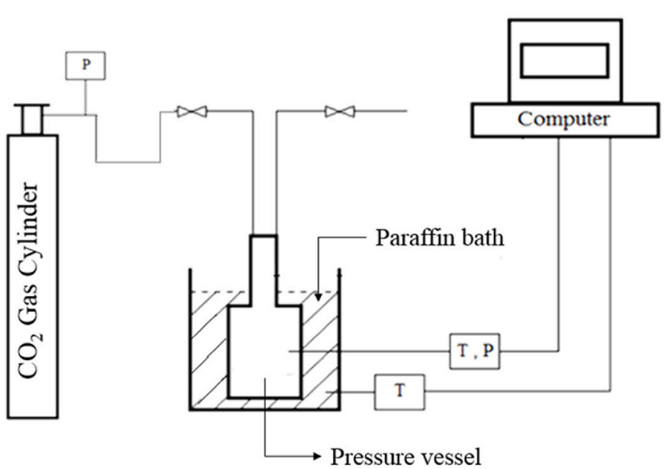

Fig. 2. Schematic view of the supercritical dryer laboratory device.

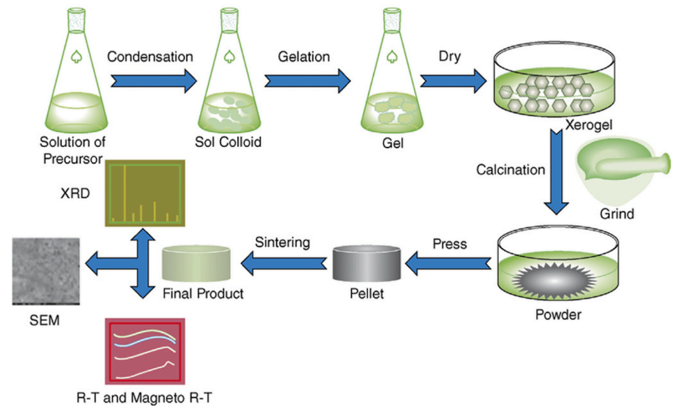

Fig. 3. Flow chart for the preparation of alumina gel by sol-gel method [2].

2.5. Vacuum pump

In order to remove the liquid and gas inside the reactor, a vacuum pump is used, which can create a vacuum of about 0.5 bar in the reactor and remove the gas and liquid in the reactor.

2.6. Materials

aluminum tri-sec-butoxide 97% by weight with the chemical formula Al (OC4H9)3, prepared from Merck, Germany, was used as a precursor in the synthesis of alumina gel. 69% weight nitric acid from Merck was used as a catalyst for the hydrolysis and polymerization reaction, and pure acetic acid from Merck was also used for comparison. Deionized water for the hydrolysis of Aluminum tri sec_ butoxide, Deionized water obtained from Zalal Company of Iran was used.

2.7. Experiment method

2.7.1. Preparation of gel with One step hydrolysis

In this method, first the solvent was poured into the test vessel using a pipette and stirred with Aluminum tri sec_ butoxide (ASB) for 15 min to obtain a homogeneous solution of the solvent and precursor. Then, during 45 min, double distilled water along with solvent was added drop by drop to the initial solution. The temperature of the hydrolysis reaction was controlled using a paraffin bath and a thermometer. First, the hydrolysis proceeds slowly and the solution becomes a little lighter than before. with adding nitric acid 69% weight as a catalyst drop by drop, the hydrolysis reaction happens quickly. Fig. 3 the flow chart for the preparation of production of alumina gel.

2.7.2. Preparation of gel with two step hydrolysis

This method is exactly like one-step hydrolysis, with the difference that after adding water and solvent, the solution is stirred for 15 min, then water and solvent are added drop by drop over 30 minutes, and in this way two the hydrolysis step takes place [71–73,101–104]. Then

Table 1
One-step and two-step hydrolysis of alumina gel synthesis with a concentration of 16% weight of precursor to solvent.

Experiment number	1	2
Hydrolysis step	One-step	two-step
Initial concentration of precursor (weight percent)	16	16
The amount of water in the first step (ml)	0.16	0.1
The amount of ethanol in the first step (ml)	1.6	0.6
The amount of water in the second stage (ml)	0	0.06
Hydrolysis reaction temperature (°C)	0	1
Amount of acid (ml)	32	32
Gel formation temperature (°C)	0.25	0.25
Initial concentration of precursor (weight percent)	70	70

Table 2
Different amounts of acid in gel synthesis with a concentration of 16% weight of the precursor to the solvent in the initial solution and one-step hydrolysis.

Experiment number	Volume of acid added (ml)	Molar ratio of water to precursor	Hydrolysis temperature (C)
3	02/0	2	32
4	1/0	2	32
5	2/0	2	32
6	4/0	2	32
7	5/0	2	32

Table 3
Different values of the molar ratio of water to precursor with a concentration of 16% weight of precursor to solvent in the initial solution by one-step hydrolysis method.

Experiment number	Volume of acid added (ml)	Molar ratio of water to precursor	Hydrolysis temperature (C)
8	0.1	2	32
9	0.1	3	32
10	0.1	7	32
11	0.1	10	32

acid is added and a clear gel is obtained and finally a gel is formed at 70 °C or at ambient temperature. The hydrolysis temperature in the two stages can be considered the same or different. Alumina gel was investigated by two methods of one-step and two-step hydrolysis, synthesis and formation time of alumina gel. Table 1 shows the conditions and values used to test gel formation by two methods. In one-stage hydrolysis, 0.16 ml of water was added along with 1.6 ml of ethanol during 45 minutes, and in two-stage hydrolysis, the same amount was added in two stages during 45 and 30 min, respectively.

2.7.3. *Experiment to determine the effect of acid*

In order to determine the effect of the amount of acid on the time of gel formation, according to Table 2, the test was performed in 5 different amounts of acid, 0.02, 0.1, 0.2, 0.4 and 0.5 with an initial concentration of 16 %weight of the precursor. The sol was placed at 70 °C to form a gel. In the hydrolysis stage, 0.16 ml of water was mixed with 1.6 ml of ethanol and added to the initial solution [74–76,105–110].

2.7.4. *Experiment to determine the effect of water*

To determine the effect of the amount of water added to carry out the reaction, gel formation was done in 4 M ratios of water to precursor equal to 2, 3, 7 and 10, according to Table 3. In all 4 experiments, the precursor concentration in the initial solution was 16% weight and the gel formation temperature was 70 °C, and in the hydrolysis stage, water (with the mentioned molar ratios, compared to the precursor) with 1.6 ml Ethanol was mixed and added to the original solution [77–80, 111–115].

2.7.5. *Experiment to determine the effect of temperature*

In order to determine the effect of temperature on gel formation, hydrolysis was performed at two temperatures of 32 and 60 °C, according to Table 4. The concentration of the precursor in the initial solution in both tests was 16% weight and the temperature of gel formation was 70 °C, and in the hydrolysis stage, 0.5 ml of water was mixed with 1.6 ml of ethanol and added to the initial solution.

2.7.6. *Experiment effect of the initial concentration of the solution*

Alumina gel formation experiment was performed in three initial concentrations of 6, 10 and 16% weight of aluminum tri-sec-butoxide in ethanol.

0.16 ml of water was mixed with 1.6 ml of ethanol and added to the initial solution. The gel formation temperature is 70 °C. Other conditions are given in Table 5.

2.7.7. *Comparison experiment between nitric acid and acetic acid in hydrolysis reaction*

According to Table 6, nitric acid and acetic acid were used to increase the hydrolysis rate of aluminum tri-sec-butoxide for the formation of alumina gel, and 0.25 ml of acid was used for the hydrolysis reaction. Hydrolysis was done in two stages, the first stage at 60 °C and the second stage at ambient temperature [81–83,116–120].

2.7.8. *Drying gel*

Gel drying was done in two methods.

✓ Environmental drying: The environmental method was done by placing the gel in the environment for 30 days or placing the gel at a temperature of 100 °C in an oven for 5 h [121–123].
✓ Supercritical drying: In this method, the gel was placed on a mesh with small holes made of stainless steel, inside the reactor of the device. The reactor was closed and placed in a paraffin bath and carbon dioxide gas was injected [124–127].

Table 4
One-step hydrolysis with a concentration of 16% weight of the precursor to the solvent in the initial solution at two temperatures of 32 and 60 °C.

Experiment number	Volume of acid added (ml)	Molar ratio of water to precursor	Hydrolysis temperature(C)
12	0.1	7	32
13	0.1	7	60

Table 5
One-step hydrolysis of the precursor in different concentrations of the precursor to the solvent in the initial solution.

Experiment number	Concentration of the precursor in the initial solution (% weight)	Amount water (ml)	Amount water (ml)	Amount acid (ml)	Hydrolysis temperature (°C)
14	6	6/1	0.16	25/0	32
15	10	6/1	0.16	25/0	32
16	16	6/1	0.16	25/0	32

Table 6
Using acetic and nitric acid in two-stage hydrolysis with a concentration of 16% weight of the precursor to the solvent in the initial solution.

Experiment number	acid	First stage water (ml)	First stage ethanol (ml)	second stage water (ml)	second stage ethanol (ml)
17	acetic acid	0.1	0.6	0.06	1
18	nitric acid	0.1	0.6	0.06	1

Table 7
Results of one -step hydrolysis and two-step hydrolysis of the precursor.

Experiment number	1	2
Hydrolysis method	one -step	two-step
Gel formation time	20	15
Amount of precipitate after hydrolysis reaction	0	0
Gel volume (ml)	8.5	9

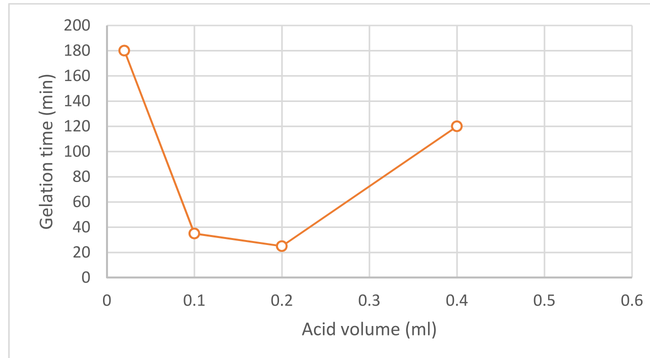

Fig. 4. Gel formation time according to the volume of acid at a molar ratio of water to precursor equal = 2 and a temperature of 32 °C.

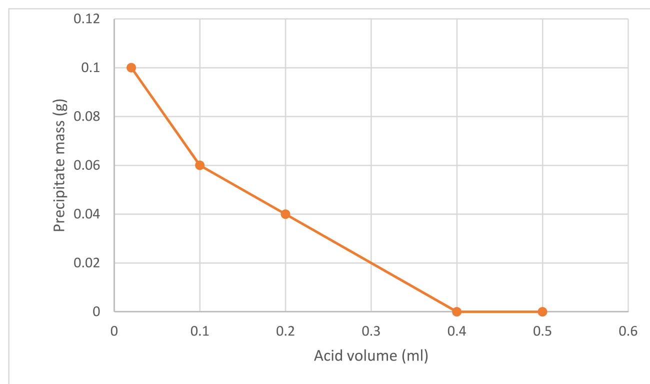

Fig. 5. The mass of sediment formed according to the volume of acid at a molar ratio of water to precursor equal = 2 and a temperature of 32 °C.

3. Results and discussion

3.1. Examining formation time of alumina gel

3.1.1. Comparison between one-step and two-step hydrolysis

Table 7 reports the results of one-stage and two-stage hydrolysis of aluminum trisecting oxide with an initial concentration of 16% weight in ethanol solvent. As the obtained results show, gel is formed faster in two-step hydrolysis, in fact, the sol had more time to complete the hydrolysis reaction.

3.1.2. Investigation effect of acid amount

The results of the tests performed in different conditions and molar ratios are reported in Table 8. As seen in Fig. 4, adding acid up to 0.2 ml increases the rate of hydrolysis and gel formation in a shorter time, but with adding more acid, gel polymerization is delayed and in 0.5 ml of acid does not form a gel. The gel formation time is optimized in the amount of 0.2 ml. Considering that the pH of the hydrolysis reaction is acidic and the pH of the condensation reaction is basic, then with adding acid, the hydrolysis will be done well, but the condensation reaction will be slower. As can be seen in Fig. 5, under the same conditions, with adding the volume of acid from 0.02 to 0.4 ml, the amount of precipitation decreases and the solution becomes more transparent. with adding the amount of 0.5 ml of sol acid, it is clear, colorless and without any sediment, but the gel is not formed. Actually, with changing the amount of acid, the thickness of the acidic layer formed around the micelle's changes. with increasing the amount of acid and as a result of increasing the thickness of the acidic layer, the amount of precipitation decreases because the formed layer prevents the micelles from sticking together and coagulation, and no precipitation occurs in the amount of 0.5 ml of acid. with increasing the thickness of the acidic layer prevents the continuation of the condensation reaction and, as a result, prevents gel formation.

3.1.3. Investigating effect of molar ratio of water to precursor

The results of the gel formation test in different molar ratios of water to precursor are reported in Table 9. As can be seen in Figs. 6 and 7, with changing the molar ratio of water to aluminum tri-sec-butoxide from 2 to 7, the amount of precipitation is created and the time of gel formation increases, and at a molar ratio of 10, alumina gel is no longer formed. with adding less than the stoichiometric amount of water to the alkoxide, we will get a better result for the gel formation time. The stoichiometric ratio of aluminum alkoxide to water in the hydrolysis reaction is equal = 3, but the results of the experiments showed that in the molar ratio of alkoxide to water equal = 2, the gel formation time is shorter and the amount of sediment created is less. Considering that water is one of the products in the condensation reaction and water is formed during the formation of water gel, this result is justified.

3.1.4. Investigating effect of temperature

From the comparison of the test results at two different temperatures of 32 and 60 °C, it was found that hydrolysis of alkoxide is better at 60 °C, because no sediment is formed after adding acid and the gel is formed in a shorter time. In fact, heat Dissolving the precursor to dissolve better in ethanol and the hydrolysis reaction is performed better. The results of hydrolysis at two temperatures of 32 and 60 °C are

Table 8
Results of the gel synthesis test in different amounts of acid.

Experiment number	Volume of acid (ml)	Molar ratio of water to precursor	Gel volume (ml)
3	0.02	2	3
4	0.1	2	7
5	0.2	2	7.5
6	0.4	2	5
7	0.5	2	0

Table 9
Results of the gel synthesis test in different molar ratios of water to precursor.

Experiment number	Molar ratio of water to precursor	Volume of acid added(ml)	Gel volume(ml)
8	2	0.1	7
9	3	0.1	6.5
10	7	0.1	2.5
11	10	0.1	0

reported in Table 10.

3.1.5. Investigating effect of the initial concentration of the solution

The results of the gel formation test in three different weight ratios of precursor to ethanol in the initial solution are shown in Table 11. The results show that the initial concentration of the precursor in the solution has no effect on the amount of sediment left in the container after adding acid, and taking into account the error in measuring the mass of the sediment, almost the same amount of sediment was left in all three tests. The results indicate that alumina gel is not formed at any concentration of the precursor. As can be seen in Table 11, the alumina gel was formed only at a concentration of 16% weight of the precursor to the solvent.

3.1.6. Investigation of alumina gel drying

Alumina gel was synthesized with the optimal parameters obtained from the previous part, and after a day, when the gel bonds became stronger, it was dried in both ambient and supercritical conditions. Fig. 8 shows the temperature and pressure changes based on time during the drying Experiment in supercritical conditions. In the supercritical drying method, first the bath temperature of the dryer was set to 15 °C, then carbon dioxide gas was injected into the reactor. As the temperature of the carbon dioxide gas decreases, it begins to liquefy, and the pressure of the gas drops sharply [128–131]. To compensate for this pressure, drop, the gas inlet valve was open for 5 min at a temperature of 15 °C to keep the gas pressure at 69 bar, which was the pressure of the capsule. Then the inlet and outlet valves were closed and the temperature of the bath was set to 35 °C. At the same time as the temperature increased, the pressure also increased sharply. After half an hour, the reactor reached a temperature of 35 °C and a pressure of 130 bar, which means supercritical conditions. The reactor remained at this temperature and pressure for 4 h and then the outlet valve was opened so that the carbon dioxide gas along with the ethanol released from the gel cavities went out. The discharge was carried out at a constant temperature of 35 °C and lasted for 1h until the pressure reached 75 bar. Above the critical point, the outlet valve was closed. At this stage, the temperature and pressure were not allowed to reach below the critical point. In the next step, the temperature of the reactor was set to 45 °C so that the pressure increases with the increase in temperature. The reactor reached a temperature of 45 °C and a pressure of 100 bar within 45 min. The reactor and gel remained in this condition for 5h and finally the reactor was completely drained. Alumina gel was dried in the supercritical conditions of the device and under the mentioned process during a period of 10 h, and alumina aerogel was obtained. The resulting aerogel and xerogel were photographed using a scanning electron microscope [132–136]. The image related to SEM analysis indicate that when the gel

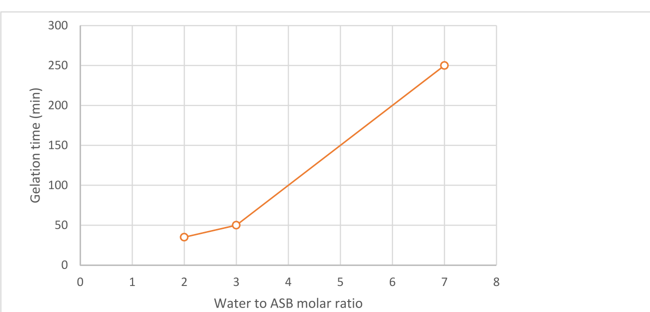

Fig. 6. Gel formation time according to the molar ratio of water to precursor at a temperature of 32 °C and 0.5 ml of nitric acid.

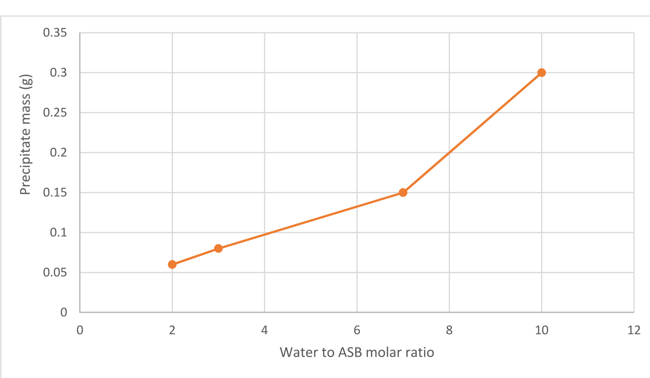

Fig. 7. The mass of sediment formed according to the molar ratio of water to precursor at 32 °C and 0.5 ml of nitric acid.

Table 10
The results of hydrolysis at two temperatures of 32 and 60 °C.

Experiment number	12	13
Hydrolysis temperature (C)	60	32
Molar ratio of water to precursor	7	7
Volume of acid (ml)	0.1	0.1
Gel volume (ml)	4.5	2.5
Sediment mass (gr)	0	0.16
Gel formation time (min)	210	250

Table 11
The results of hydrolysis with different precursor concentrations.

Experiment number	14	15	16
Precursor concentration (%weight)	6	10	16
Sediment mass (gr)	0.07	0.08	0.06
Gel volume (ml)	0	0	7
Gel formation time (minutes)	–	–	35

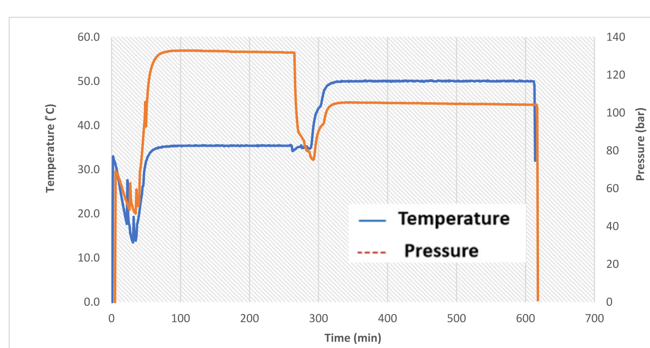

Fig. 8. Reactor temperature and pressure changes according to alumina gel drying time.

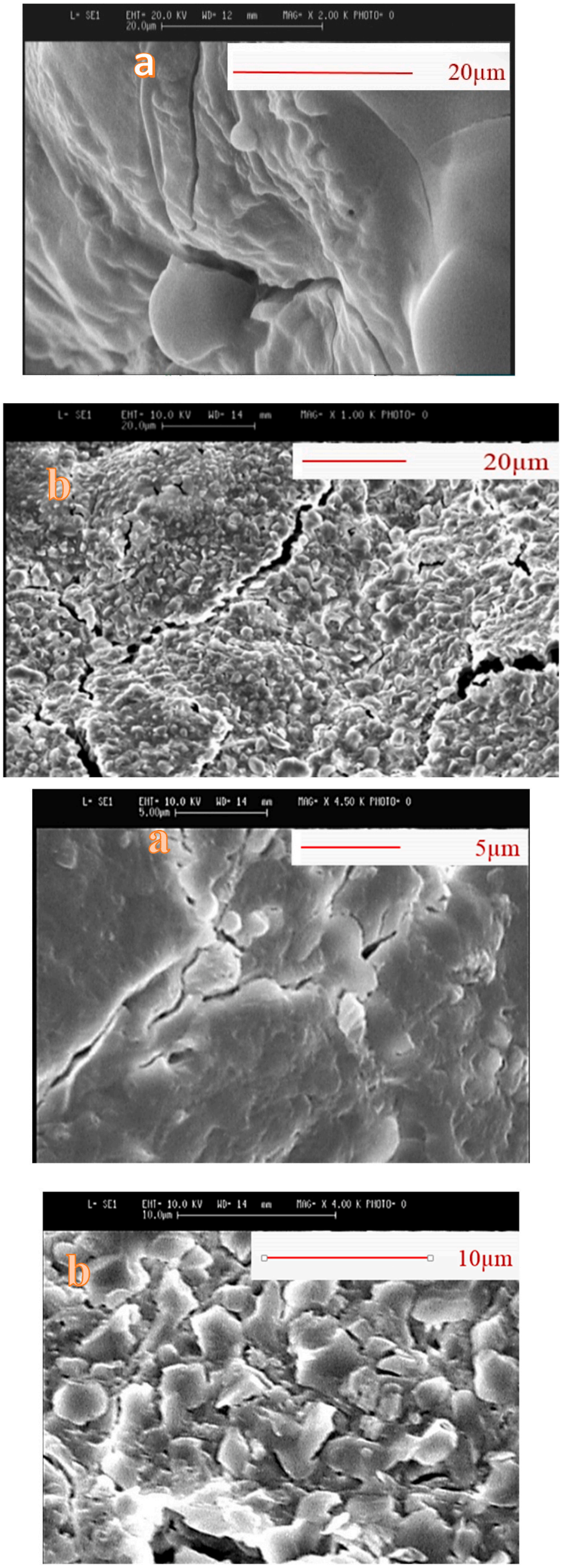

Fig. 9. SEM analysis of dried alumina gel in a) ambient condition b) supercritical condition.

is dried at ambient temperature, the holes between the solid structure of the gel disappear and the particles stick to each other, but when the gel is dried in supercritical conditions, it is possible that the solid structure of the gel is not destroyed and the holes and voids are preserved. As seen in the SEM analysis of the aerogel, there are cavities between the different surfaces of the solid structure of the gel (Fig. 9). In the drying method with a simple process of evaporation and removal of the solvent at atmospheric pressure, due to the capillary forces created by the interaction between the two phases of liquid and vapor, due to the evaporation of the solvent, part of the volume of the holes is lost and as a result, the porosity decreases. In fact, the way to deal with this problem is to remove the contact surface between the gas and liquid phase, considering that the surface tension of the material becomes zero at the supercritical point, the drying method in supercritical conditions solves this problem by removing the capillary forces. The solid structure of the gel is maintained and the porosity is not lost.

4. Conclusion

In this research, synthesis of alumina gel as a support for nanocatalysts through hydrolysis of aluminum tri-sec-butoxide (ASB) in ethanol was investigated. The gel synthesis was carried out at 32 and 60 °C with different concentrations of water and precursor and different types and amounts of acid as catalyst. Rate of gel formation, efficiency of hydrolysis and polymerization and amount of gel production were measured and discussed. Results showed that acid addition around 0.2 ml and water to ASB malar ratio of 2 at 60 °C maximized the amount of gel produced and minimized the gelation time. The results showed that adding 0.2 ml of nitric acid per 1 ml of aluminum tri-sec-butoxide in a solution of 16% weight of aluminum tri-sec-butoxide and the molar ratio of water to precursor is equal = 2, at a temperature of 60 °C, the amount of gel and the time of formation of alumina gel are optimal and the maximum amount of gel is obtained in the shortest possible time. Next, the alumina gel was dried by two ambient and supercritical methods, and the scanning electron microscope analysis of the product showed that in the supercritical method, due to the elimination of capillary forces, the pores of the gel are preserved, and the alumina obtained by this method is very suitable for use as a catalyst base.

Author contributions

Rusul Alabada, Mustafa M. Kadhim, Zainab sabri Abbas, Ahmed Mahdi Rheima, Usama S. Altimari: reviewing and editing. Ashour H. Dawood, Alaa dhari jawad al-bayati, Zainab Talib Abed, Rusul Saeed Radhi, Asala Salam Jaber, Safa K. Hachim, Farah K. Ali, Zaid H. Mahmoud: reviewing and editing. Ehsan Kianfar: Investigation, writing – original draft, reviewing and editing.

Ethical approval

Not applicable.

Consent for publication

Not applicable.

Availability of data and material

Not applicable.

Funding

Not applicable.

Declaration of competing interest

The authors declare that they have no known competing financial interests or personal relationships that could have appeared to influence the work reported in this paper.

Data availability

The data that has been used is confidential.

Abbreviation

(ASB) aluminum tri-sec-butoxide
(SiCl4) silicon tetrachloride
(XRD) X-ray diffraction

References

[1] S. Mersagh Dezfuli, M. Sabzi, Deposition of self-healing thin films by the sol–gel method: a review of layer-deposition mechanisms and activation of self-healing mechanisms, Appl. Phys. A 125 (8) (2019) 557.
[2] B.E. Yoldas, Alumina gels that form porous transparent Al 2 O 3, J. Mater. Sci. 10 (1975) 1856–1860.
[3] B.E. Yoldas, B.E. Yoldas, Hydrolysis of aluminium alkoxides and bayerite conversion, J. Appl. Chem. Biotechnol. 23 (11) (1973) 803–809.
[4] J. Walendziewski, M. Stolarski, M.A. Steininger, B. Pniak, Synthesis and properties of alumina aerogels, React. Kinet. Catal. Lett. 66 (1999) 71–77.
[5] J. Walendziewski, M. Stolarski, Synthesis and properties of alumina aerogels (II), React. Kinet. Catal. Lett. 71 (2000) 201–207.
[6] J.F. Poco, J.H. Satcher Jr., L.W. Hrubesh, Synthesis of high porosity, monolithic alumina aerogels, J. Non-Cryst. Solids 285 (1-3) (2001) 57–63.
[7] L. Le Bihan, F. Dumeignil, E. Payen, J. Grimblot, Chemistry of preparation of alumina aerogels in presence of a complexing agent, J. Sol. Gel Sci. Technol. 24 (2002) 113–120.
[8] P.K. Sharma, V.V. Varadan, V.K. Varadan, A critical role of pH in the colloidal synthesis and phase transformation of nano size α-Al2O3 with high surface area, J. Eur. Ceram. Soc. 23 (5) (2003) 659–666.
[9] M.S. Bono, A.M. Anderson, M.K. Carroll, Alumina aerogels prepared via rapid supercritical extraction, J. Sol. Gel Sci. Technol. 53 (2010) 216–226.
[10] M. Sabzi, S.H.M. Anijdan, M. Roghani Zadeh, M. Farzam, The effect of heat treatment on corrosion behaviour of Ni–P–3 gr/lit Cu nano-composite coating, Can. Metall. Q. 57 (3) (2018) 350–357.
[11] T.R. Tamilarasan, U. Sanjith, M.S. Shankar, G. Rajagopal, Effect of reduced graphene oxide (rGO) on corrosion and erosion-corrosion behaviour of electroless Ni-P coatings, Wear 390 (2017) 385–391.
[12] A.S. Selvakumar, B. Surya Rajan, M.A. Sai Balaji, B. Selvaraj, Strain analysis of AA6063 aluminum alloy by tube hydroforming process, in: Advances in Manufacturing Processes: Select Proceedings of ICEMMM 2018, Springer Singapore, 2019, pp. 13–21.
[13] M. Sabzi, S. Mersagh Dezfuli, Deposition of Al2O3 ceramic film on copper-based heterostructured coatings by aluminizing process: study of the electrochemical responses and corrosion mechanism of the coating, Int. J. Appl. Ceram. Technol. 16 (1) (2019) 195–210.
[14] S.M. Dezfuli, M. Sabzi, Effect of yttria and benzotriazole doping on wear/corrosion responses of alumina-based nanostructured films, Ceram. Int. 44 (16) (2018) 20245–20258.
[15] M. Sabzi, S.M. Dezfuli, S.M. Mirsaeedghazi, The effect of pulse-reverse electroplating bath temperature on the wear/corrosion response of Ni-Co/tungsten carbide nanocomposite coating during layer deposition, Ceram. Int. 44 (16) (2018) 19492–19504.
[16] M. Sabzi, S.M. Far, S.M. Dezfuli, Characterization of bioactivity behavior and corrosion responses of hydroxyapatite-ZnO nanostructured coating deposited on NiTi shape memory alloy, Ceram. Int. 44 (17) (2018) 21395–21405.
[17] S.H. Mousavi Anijdan, M. Sabzi, M. Asadian, H.R. Jafarian, Effect of sub-layer temperature during HFCVD process on morphology and corrosion behavior of tungsten carbide coating, Int. J. Appl. Ceram. Technol. 16 (1) (2019) 243–253.
[18] S. Raghunandan, R.S. Kumar, M. Kamaraj, A.S. Gandhi, Role of water in the sol-gel synthesis of yttrium monosilicate, Ceram. Int. 45 (4) (2019) 4487–4492.
[19] M. Sabzi, S.M. Anijdan, Microstructural analysis and optical properties evaluation of sol-gel heterostructured NiO-TiO2 film used for solar panels, Ceram. Int. 45 (3) (2019) 3250–3255.
[20] A.S. Sihar, N.H. Alias, M.Z. Shahruddin, S.S.A. Syed Hassan, N.R.N. Him, N. H. Othman, Sol-gel-derived perovskite-based sorbents for high-temperature air separation, J. Sol. Gel Sci. Technol. 89 (2019) 776–784.
[21] S. Palanichamy, J.R. Mohamed, K.D.A. Kumar, M. Anitha, S. Pandiarajan, L. Amalraj, Effect of molar concentration on physical properties of spraydeposited SnO 2 thin films using nebulizer, J. Sol. Gel Sci. Technol. 89 (2019) 392–402.
[22] A. Dey, S. Roy, S.K. Sarkar, Synthesis, fabrication and characterization of ZnO-based thin films prepared by sol–gel process and H 2 gas sensing performance, J. Mater. Eng. Perform. 27 (2018) 2701–2707.
[23] K. Seema, B. Uma, K. Suchita, Transformations in sol-gel synthesized nanoscale hydroxyapatite calcined under different temperatures and time conditions, J. Mater. Eng. Perform. 21 (2012) 1737–1743.
[24] R.B. Vignesh, T.N.J.I. Edison, M.G. Sethuraman, Sol–gel coating with 3-mercaptopropyltrimethoxysilane as precursor for corrosion protection of aluminium metal, J. Mater. Sci. Technol. 30 (8) (2014) 814–820.
[25] B. Tlili, A. Barkaoui, Effect of sol-gel coating on friction and thermomechanical wear, Int. J. Adv. Des. Manuf. Technol. 89 (2017) 1799–1811.
[26] M.M. Akmal, A.R.M. Warikh, U.A.A. Azlan, N.A. Azmi, M.S. Salleh, M.S. Kasim, Optimizing the processing conditions of sodium potassium niobate thin films prepared by sol-gel spin coating technique, Ceram. Int. 44 (1) (2018) 317–325.
[27] H.Y. Su, P.L. Chen, C.S. Lin, Sol–gel coatings doped with organosilane and cerium to improve the properties of hot-dip galvanized steel, Corrosion Sci. 102 (2016) 63–71.
[28] R.V. Lakshmi, G. Yoganandan, A.V.N. Mohan, B.J. Basu, Effect of surface pretreatment by silanization on corrosion protection of AA2024-T3 alloy by sol–gel nanocomposite coatings, Surf. Coating. Technol. 240 (2014) 353–360.
[29] A.N.D. Krupa, R. Vimala, Evaluation of tetraethoxysilane (TEOS) sol–gel coatings, modified with green synthesized zinc oxide nanoparticles for combating microfouling, Mater. Sci. Eng. C 61 (2016) 728–735.
[30] V. Moutarlier, B. Neveu, M.P. Gigandet, Evolution of corrosion protection for sol–gel coatings doped with inorganic inhibitors, Surf. Coating. Technol. 202 (10) (2008) 2052–2058.
[31] J. Mosa, N.C. Rosero-Navarro, M. Aparicio, Active corrosion inhibition of mild steel by environmentally-friendly Ce-doped organic–inorganic sol–gel coatings, RSC Adv. 6 (46) (2016) 39577–39586.
[32] N. Kumar, R. Subasri, Corrosion protection and self-healing by sol-gel process: a review of recent patent literature, Recent Pat. Corros. Sci. 2 (2) (2012) 148–163.
[33] R.N. Chauhan, Structural and optical properties of sol-gel derived Zn1− xTixO1+ x nanoparticles, Mater. Lett. 245 (2019) 178–182.
[34] M. Asadian, M. Sabzi, S.M. Anijdan, The effect of temperature, CO2, H2S gases and the resultant iron carbonate and iron sulfide compounds on the sour corrosion behaviour of ASTM A-106 steel for pipeline transportation, Int. J. Pres. Ves. Pip. 171 (2019) 184–193.
[35] T.R. Tamilarasan, R. Sathish Kumar, R. Rajendran, G. Rajagopal, Optimization of electroless Ni-P-nano-TiO2 Coating parameters using Taguchi method for corrosion performance, in: Applied Mechanics and Materials, vol. 813, 2015, pp. 95–100 (Trans Tech Publications Ltd).
[36] D. Bokov, A. Turki Jalil, S. Chupradit, W. Suksatan, M. Javed Ansari, I. H. Shewael, E. Kianfar, Nanomaterial by sol-gel method: synthesis and application, 2021, Adv. Mater. Sci. Eng. (2021) 1–21.
[37] K. Ehsan, Nanozeolites: synthesized, properties, applications, J. Sol. Gel Sci. Technol. 91 (2019) 415–429.
[38] M. Yang, C. Li, Y. Zhang, D. Jia, X. Zhang, Y. Hou, R. Li, J. Wang, Maximum undeformed equivalent chip thickness for ductile-brittle transition of zirconia ceramics under different lubrication conditions, Int. J. Mach. Tool Manufact. 122 (2017) 55–65.
[39] J. Zhang, C. Li, Y. Zhang, M. Yang, D. Jia, G. Liu, Y. Hou, R. Li, N. Zhang, Q. Wu, H. Cao, Experimental assessment of an environmentally friendly grinding process using nanofluid minimum quantity lubrication with cryogenic air, J. Clean. Prod. 193 (2018) 236–248.
[40] B. Li, C. Li, Y. Zhang, Y. Wang, D. Jia, M. Yang, Grinding temperature and energy ratio coefficient in MQL grinding of high-temperature nickel-base alloy by using different vegetable oils as base oil, Chin. J. Aeronaut. 29 (4) (2016) 1084–1095. CNKI:SUN:HKXS.0.2016-04-023.
[41] T. Gao, Y. Zhang, C. Li, Y. Wang, Y. Chen, Q. An, S. Sharma, Fiber-reinforced composites in milling and grinding: machining bottlenecks and advanced strategies, Front. Mech. Eng. 17 (2) (2022) 24.
[42] X. Wang, C. Li, Y. Zhang, Z. Said, S. Debnath, S. Sharma, T. Gao, Influence of texture shape and arrangement on nanofluid minimum quantity lubrication turning, Int. J. Adv. Des. Manuf. Technol. 119 (1-2) (2022) 631–646.
[43] X. Cui, C. Li, Y. Zhang, Z. Said, S. Debnath, S. Sharma, R. Li, Grindability of titanium alloy using cryogenic nanolubricant minimum quantity lubrication, J. Manuf. Process. 80 (2022) 273–286.
[44] X. Wang, C. Li, Y. Zhang, H.M. Ali, S. Sharma, R. Li, X. Liu, Tribology of Enhanced Turning Using Biolubricants: A Comparative Assessment, Tribology International, 2022, 107766.
[45] W. Xu, C.H. Li, Y. Zhang, H.M. Ali, S. Sharma, R. Li, Z. Zhou, Electrostatic atomization minimum quantity lubrication machining: from mechanism to application, Int. J. Extrem. Manuf. (2022).
[46] L.I.U. Mingzheng, L.I. Changhe, Y. Zhang, Y.A.N.G. Min, G.A.O. Teng, C.U.I. Xin, S. Sharma, Analysis of grinding mechanics and improved grinding force model based on randomized grain geometric characteristics, Chin. J. Aeronaut. (2022).
[47] D. Liu, C. Li, L. Dong, A. Qin, Y. Zhang, M. Yang, S. Sharma, Kinematics and improved surface roughness model in milling, Int. J. Adv. Des. Manuf. Technol. (2022) 1–22.
[48] M. Liu, C. Li, Y. Zhang, M. Yang, T. Gao, X. Cui, S. Sharma, Analysis of grain tribology and improved grinding temperature model based on discrete heat source, Tribol. Int. 180 (2023), 108196.
[49] X. Wang, Y. Song, C. Li, Y. Zhang, H.M. Ali, S. Sharma, Z. Zhou, Nanofluids application in machining: a comprehensive review, Int. J. Adv. Des. Manuf. Technol. (2023) 1–52.
[50] E. Vafa, R. Bazargan-lari, M.E. Bahrololoom, A.M. Amani, Effect of polyvinyl alcohol concentration on biomedical application of chitosan/bioactive glass composite coated on AZ91D magnesium alloy, Mater. Chem. Phys. 291 (2022), 126650.

[51] M.F. Bashir, Discovering the evolution of Pollution Haven Hypothesis: a literature review and future research agenda, Environ. Sci. Pollut. Control Ser. 29 (32) (2022) 48210–48232.
[52] E. Vafa, R. Bazargan-Lari, Bovine serum albumin protected gold nanozymes as a novel anti-cancer nanodrug for acute T-type lymphoblastic leukemia treatment via effect on the expression of anti-apoptotic genes, Appl. Biol. Chem. 64 (1) (2021) 86.
[53] S. Mitura, A. Sionkowska, A. Jaiswal, Biopolymers for hydrogels in cosmetics, J. Mater. Sci. Mater. Med. 31 (2020) 1–14.
[54] F. Heidari, R. Bazargan-Lari, M. Razavi, F. Fahimipour, D. Vashaee, L. Tayebi, Nano-hydroxyapatite and nano-hydroxyapatite/zinc oxide scaffold for bone tissue engineering application, Int. J. Appl. Ceram. Technol. 17 (6) (2020) 2752–2761.
[55] A. Najafi, F. Sharifi, S. Mesgari-Abbasi, G. Khalaj, Influence of pH and temperature parameters on the sol-gel synthesis process of meso porous ZrC nanopowder, Ceram. Int. 48 (18) (2022) 26725–26731.
[56] O. Fakhimi, A. Najafi, G. Khalaj, A facile rout to obtain Al2O3 nanopowder via recycling aluminum cans by sol-gel method, Mater. Res. Express 7 (4) (2020), 045008.
[57] M. Rahmani-Azad, A. Najafi, N. Rahmani-Azad, G. Khalaj, Improvement of ZrB2 nanopowder synthesis by sol-gel method via zirconium alkoxide/boric acid precursors, J. Sol. Gel Sci. Technol. 103 (1) (2022) 87–96.
[58] F. Sharifi, Z. Mahmoodi, S.M. Abbasi, A. Najafi, G. Khalaj, Synthesis and characterization of mesoporous TiC nanopowder/nanowhisker with low residual carbon processed by sol–gel method, J. Mater. Res. Technol. 22 (2023) 2462–2472.
[59] A. Najafi, F. Golestani-Fard, H.R. Rezaie, Improvement of SiC nanopowder synthesis by sol–gel method via TEOS/resin phenolic precursors, J. Sol. Gel Sci. Technol. 75 (2015) 255–263.
[60] A. Najafi, F. Golestani-Fard, H.R. Rezaie, N. Ehsani, Effect of APC addition on stability of nanosize precursors in sol–gel processing of SiC nanopowder, J. Alloys Compd. 505 (2) (2010) 692–697.
[61] E. Myrovali, in: Magnetic Nanoparticle Arrays: Features, Properties, Applications (Doctoral Dissertation, Αριστοτέλειο Πανεπιστήμιο Θεσσαλονίκης (ΑΠΘ), 2020 (Σχολή Θετικών Επιστημών. Τμήμα Φυσικής)).
[62] A. Najafi, F. Golestani-Fard, H.R. Rezaie, S.P. Saeb, Sol-Gel synthesis and characterization of SiC–B4C nano powder, Ceram. Int. 47 (5) (2021) 6376–6387.
[63] A. Najafi, F. Golestani-Fard, H.R. Rezaie, Sol-gel synthesis and characterization of B4C nanopowder, Ceram. Int. 44 (17) (2018) 21386–21394.
[64] S. Altınok, *Thermal Plasma Synthesis of Boron carbide*(Master's Thesis, Middle East Technical University, 2018.
[65] A. Najafi, F. Golestani-Fard, H.R. Rezaie, N. Ehsani, A study on sol–gel synthesis and characterization of SiC nano powder, J. Sol. Gel Sci. Technol. 59 (2011) 205–214.
[66] A. Najafi, F.G. Fard, H.R. Rezaie, N. Ehsani, Synthesis and characterization of SiC nano powder with low residual carbon processed by sol–gel method, Powder Technol. 219 (2012) 202–210.
[67] U. Abdul-Reda Hussein, Z.H. Mahmoud, K.M. Abd Alaziz, M.L. Alid, Y. Yasin, F. K. Ali, E. Kianfar, Antimicrobial finishing of textiles using nanomaterials, Braz. J. Biol. 84 (2023), e264947.
[68] Z.H. Mahmoud, H.A. Salman, H.H. Hussein, A.H. Adhab, K. Al-Majdi, T. Rasheed, E. Kianfar, Organic chemical Nano sensors: synthesis, properties, and applications, Braz. J. Biol. 84 (2023), e268893.
[69] I. Raya, H.H. Kzar, Z.H. Mahmoud, A. Al Ayub Ahmed, A.Z. Ibatova, E. Kianfar, A review of gas sensors based on carbon nanomaterial, Carbon Lett. (2021) 1–26.
[70] Z.H. Mahmoud, A. Hamrouni, A.B. Kareem, M.A. Mostafa, A.H. Majeed, Synthesis and characterization of chitosan sheet modified by varied weight ratio of anatase (TiO2) nano mixture with Cr (VI) adsorbing, Kuwait J. Sci. (2023).
[71] M.A. Mahdi, M.A. Farhan, Z.H. Mahmoud, A.M. Rheima, Z. sabri Abbas, M. M. Kadhim, A.H. Ismail, Direct sunlight photodegradation of Congo red in aqueous solution by TiO2/rGO binary system: experimental and DFT study, Arab. J. Chem. (2023), 104992.
[72] W.A. Siswanto, R.M. Romero-Parra, R. Sivaraman, A. Turki Jalil, M.A. Gatea, M. S. Alhassan, Z.H. Mahmoud, The characterization of plastic behavior and mechanical properties in the gradient nanostructured copper, in: Proceedings of the Institution of Mechanical Engineers, Part L: Journal of Materials: Design and Applications, 2023, 14644207231161752.
[73] Z.H. Mahmoud, J.M. Mahmood, N.S. Al-Obaidi, A.M. Rahima, Gama-Fe2O3 silica-coated 2-(2-benzothiazolyl azo)-4-methoxyaniline for supercapacitive performance: original scientific paper, J. Electrochem. Sci. Eng. (2023).
[74] Z.H. Mahmoud, A.B. Mahdi, Y.S. Alnassar, H.N.K. Al-Salman, Formulation and sustained-release of verapamil hydrochloride tablets, Chemist 76 (2023).
[75] Z.H. Mahmoud, O.G. Hammoudi, A.N. Abd, Y.M. Ahmed, U.S. Altimari, A. H. Dawood, R. Shaker, Functionalize cobalt ferrite and ferric oxide by nitrogen organic compound with high supercapacitor performance, Results Chem. 5 (2023), 100936.
[76] N.S. Al-Obaidi, Z.E. Sadeq, Z.H. Mahmoud, A.N. Abd, A.S. Al-Mahdawi, F.K. Ali, Synthesis of chitosan-TiO2 nanocomposite for efficient Cr (VI) removal from contaminated wastewater sorption kinetics, thermodynamics and mechanism, J. Oleo Sci. 72 (3) (2023) 337–346.
[77] S.A. Jasim, M.H. Ali, Z.H. Mahmood, M. Rudiansyah, F.H. Alsultany, Y. F. Mustafa, A. Surendar, Role of alloying composition on mechanical properties of CuZr metallic glasses during the nanoindentation process, Met. Mater. Int. 28 (9) (2022) 2075–2082.
[78] D.O. Bokov, Y.F. Mustafa, Z.H. Mahmoud, W. Suksatan, M.A. Jawad, T. Xu, Cr-SiNT, Mn-SiNT, Ti-C70 and Sc-CNT as effective catalysts for CO2 reduction to CH3OH, Silicon 14 (14) (2022) 8493–8503.
[79] S.A. Jasim, W.K. Abdelbasset, K. Hachem, M.M. Kadhim, G. Yasin, M.A. Obaid, Z. H. Mahmoud, Novel Gd2O3/SrFe12O19@ Schiff base chitosan (Gd/SrFe@ SBCs) nanocomposite as a novel magnetic sorbent for the removal of Pb (II) and Cd (II) ions from aqueous solution, J. Chin. Chem. Soc. 69 (7) (2022) 1079–1087.
[80] Z.H. Mahmoud, R.A. AL-Bayati, A.A. Khadom, The efficacy of samarium loaded titanium dioxide (Sm: TiO2) for enhanced photocatalytic removal of rhodamine B dye in natural sunlight exposure, J. Mol. Struct. 1253 (2022), 132267.
[81] I. Raya, A.A. Mansoor Al Sarraf, G. Widjaja, S. Ghazi Al-Shawi, M. F Ramadan, Z. H. Mahmood, H. Ghaleb Maabreh, ZnMoO4 nanoparticles: novel and facile synthesis, characterization, and photocatalytic performance, J. Nanostruct. 12 (2) (2022) 446–454.
[82] Z.H. Mahmood, M. Jarosova, H.H. Kzar, P. Machek, M. Zaidi, A. Dehno Khalaji, M.M. Kadhim, Synthesis and characterization of Co3O4 nanoparticles: application as performing anode in Li-ion batteries, J. Chin. Chem. Soc. 69 (4) (2022) 657–662.
[83] A. Bahadoran, M.K. Jabarabadi, Z.H. Mahmood, D. Bokov, B.J. Janani, A. Fakhri, Quick and sensitive colorimetric detection of amino acid with functionalized-silver/copper nanoparticles in the presence of cross linker, and bacteria detection by using -template nanoparticles as peroxidase activity, Spectrochim. Acta Mol. Biomol. Spectrosc. 268 (2022), 120636.
[84] E. Kianfar, The effects of SiO2/Al2O3 and H2O/Al2O3 molar ratios on SAPO-34 catalyst in the methanol to olefin process, Silicon 15 (1) (2023) 381–396.
[85] G.F. Smaisim, K.J. Mohammed, S.K. Hadrawi, H. Koten, E. Kianfar, Properties and application of nanostructure in liquid crystals, BioNano Sci. (2023) 1–21.
[86] A. Abderrahmane, A. Mourad, S. Mohammed, G.F. Smaisim, D. Toghraie, A. Koulali, O. Younis, Second law analysis of a 3D magnetic buoyancy-driven flow of hybrid nanofluid inside a wavy cubical cavity partially filled with porous layer and non-Newtonian layer, Ann. Nucl. Energy 181 (2023), 109511.
[87] Y. Wang, J. Zheng, G.F. Smaisim, D. Toghraie, Molecular dynamics simulation of phase transition procedure of water-based nanofluid flow containing CuO nanoparticles, Alex. Eng. J. 61 (12) (2022) 12453–12461.
[88] M. Xiao, G.F. Smaisim, Joint chance-constrained multi-objective optimal function of multi-energy microgrid containing energy storages and carbon recycling system, J. Energy Storage 55 (2022), 105842.
[89] A. Mourad, A. Aissa, A.M. Abed, G.F. Smaisim, D. Toghraie, M.A. Fazilati, A. A. Alizadeh, The numerical analysis of the melting process in a modified shell-and-tube phase change material heat storage system, J. Energy Storage 55 (2022), 105827.
[90] G.F. Smaisim, A.M. Abed, H. Alavi, Analysis of pollutant emission reduction in a coal power plant using renewable energy, Int. J. Low Carbon Technol. (2022).
[91] A. Abderrahmane, W. Jamshed, A.M. Abed, G.F. Smaisim, K. Guedri, O.A. Akbari, S. Baghaei, Heat and mass transfer analysis of non-Newtonian power-law nanofluid confined within annulus enclosure using Darcy-Brinkman-Forchheimer model, Case Stud. Therm. Eng. (2022), 102569.
[92] X. Tan, R.F. Obaid, G.F. Smaisim, M.M. Esfahani, F. Alsaikhan, S. Baghaei, A. Yadav, Investigation of addition of calcium phosphate ceramic to multilayer scaffold for bone applications with improved mechanical properties: fuzzy logic analysis, Ceram. Int. (2022).
[93] S. Mir, A.M. Abed, O.A. Akbari, A. Mohammadian, D. Toghraie, A. Marzban, G. F. Smaisim, Effects of curvature existence, adding of nanoparticles and changing the circular minichannel shape on behavior of two-phase laminar mixed convection of Ag/water nanofluid, Alex. Eng. J. (2022).
[94] B. Ruhani, M.T. Andani, A.M. Abed, N. Sina, G.F. Smaisim, S.K. Hadrawi, D. Toghraie, Statistical modeling and investigation of thermal characteristics of a new nanofluid containing cerium oxide powder, Heliyon 8 (11) (2022), e11373.
[95] W. Cai, R. Sabetvand, A.M. Abed, D. Toghraie, M. Hekmatifar, A. Rahbari, G. F. Smaisim, Thermal analysis of hydration process in the vicinity of the Copper matrix using molecular dynamics simulation for application in thermal engineering, Energy Rep. 8 (2022) 7468–7475.
[96] A. Moarrefzadeh, M.R. Morovvati, S.N. Angili, G.F. Smaisim, A. Khandan, D. Toghraie, Fabrication and finite element simulation of 3D printed poly L-lactic acid scaffolds coated with alginate/carbon nanotubes for bone engineering applications, Int. J. Biol. Macromol. (2022).
[97] T. Hai, A. Abidi, L. Wang, A.M. Abed, M.Z. Mahmoud, E.M.T. El Din, G. F. Smaisim, Simulation of solar thermal panel systems with nanofluid flow and PCM for energy consumption management of buildings, J. Build. Eng. 58 (2022), 104981.
[98] G. Fadhil Smaisim, A.M. Abed, S.K. Hadrawi, A. Shamel, Parametric investigation of thermal behaviour of salt-gradient solar pool for climatic conditions, Clean Energy 6 (5) (2022) 693–704.
[99] G.F. Smaisim, M. Gholami, D. Toghraie, M. Hashemian, A.M. Abed, Numerical investigation of the flow and heat transfer of Al2O3/water nanofluid in a tube equipped with stationary and self-rotating twisted tapes, Prog. Nucl. Energy 151 (2022), 104335.
[100] Y. Jiang, G.F. Smaisim, M.Z. Mahmoud, Z. Li, H.Ş. Aybar, A.M. Abed, Simultaneous numerical investigation of the passive use of phase-change materials and the active use of a nanofluid inside a rectangular duct in the thermal management of lithium-ion batteries, J. Power Sources 541 (2022), 231610.
[101] M.W. Tian, A.M. Abed, S.R. Yan, S.M. Sajadi, M.Z. Mahmoud, H.Ş. Aybar, G. F. Smaisim, Economic cost and numerical evaluation of cooling of a cylindrical lithium-ion battery pack using air and phase change materials, J. Energy Storage 52 (2022), 104925.

[102] K.A.M. Alharbi, G.F. Smaisim, S.M. Sajadi, M.A. Fagiy, H.Ş. Aybar, S.E. Elkhatib, Numerical study of lozenge, triangular and rectangular arrangements of lithium-ion batteries in their thermal management in a cooled-air cooling system, J. Energy Storage 52 (2022), 104786.
[103] W. Wu, G.F. Smaisim, S.M. Sajadi, M.A. Fagiry, Z. Li, M.A. Shamseldin, H.Ş. Aybar, Impact of phase change material-based heatsinks on lithium-ion battery thermal management: a comprehensive review, J. Energy Storage 52 (2022), 104874.
[104] M.W. Tian, G.F. Smaisim, S.R. Yan, S.M. Sajadi, M.Z. Mahmoud, H.Ş. Aybar, A. M. Abed, Economic cost and efficiency analysis of a lithium-ion battery pack with the circular and elliptical cavities filled with phase change materials, J. Energy Storage 52 (2022), 104794.
[105] W. Brontowiyono, W.A. AbdulHussein, G.F. Smaisim, M.Z. Mahmoud, S. Singh, H. A. Lafta, S. Aravindhan, Annealing temperature effect on structural, magnetic properties and methyl green degradation of Fe2O3 nanostructures, Arabian J. Sci. Eng. (2022) 1–8.
[106] Y. Tian, I. Patra, H.S. Majdi, N. Ahmad, R. Sivaraman, G.F. Smaisim, M. Hekmatifar, Investigation of atomic behavior and pool boiling heat transfer of water/Fe nanofluid under different external heat fluxes and forces: a molecular dynamics approach, Case Stud. Therm. Eng. 38 (2022), 102308.
[107] G.F. Smaisim, H. Al-Madhhachi, A.M. Abed, Study the thermal management of Li-ion batteries using looped heat pipes with different nanofluids, Case Stud. Therm. Eng. 37 (2022), 102227.
[108] G.F. Smaisim, A.M. Abed, A. Shamel, Modeling the Thermal Performance for Different Types of Solar Chimney Power Plants, Complexity, 2022, 2022.
[109] G.F. Smaisim, M.O. Bidgoli, K.L. Goh, H. Bakhtiari, Review of thermoelastic, thermal properties and creep analysis of functionally graded cylindrical shell, Aust. J. Mech. Eng. (2022) 1–12.
[110] G.F. Smaisim, A.M. Abed, S.K. Hadrawi, A. Shamel, Modeling and thermodynamic analysis of solar collector cogeneration for residential building energy supply, J. Eng. (2022), 2022.
[111] M. Mozafarifard, A. Azimi, H. Sobhani, G.F. Smaisim, D. Toghraie, M. Rahmani, Numerical study of anomalous heat conduction in absorber plate of a solar collector using time-fractional single-phase-lag model, Case Stud. Therm. Eng. 34 (2022), 102071.
[112] Z.M. Sharba, G.F. Smaisim, A.A.A. Arani, Thermal performance of inline and staggered bank of tubes with laminar cross flow, in: 2022 5th International Conference on Engineering Technology and its Applications (IICETA), 2022, May, pp. 77–84.
[113] G.F. Smaisim, N.M. Prabu, A.P. Senthilkumar, A.M. Abed, Synthesis of biodiesel from fish processing waste by nano magnetic catalyst and its thermodynamic analysis, Case Stud. Therm. Eng. (2022), 102115.
[114] W.A. AbdulHussein, A.M. Abed, D.B. Mohammed, G.F. Smaisim, S. Baghaei, Investigation of boiling process of different fluids in microchannels and nanochannels in the presence of external electric field and external magnetic field using molecular dynamics simulation, Case Stud. Therm. Eng. (2022), 102105.
[115] S. Ahamad, M. Mohseni, V. Shekher, G.F. Smaisim, A. Tripathi, J. Alanya-Beltran, A detailed analysis of the critical role of artificial intelligence in enabling high-performance cloud computing systems, in: 2022 2nd International Conference on Advance Computing and Innovative Technologies in Engineering (ICACITE), IEEE, 2022, April, pp. 156–159.
[116] A.N. Doss, D. Shah, G.F. Smaisim, M. Olha, S. Jaiswal, A comprehensive analysis of internet of things (IOT) in enhancing data security for better system integrity-A critical analysis on the security attacks and relevant countermeasures, in: 2022 2nd International Conference on Advance Computing and Innovative Technologies in Engineering (ICACITE), IEEE, 2022, April, pp. 165–167.
[117] A. Lefteh, M. Houshmand, M. Khorrampanah, G.F. Smaisim, Optimization of modified adaptive neuro-fuzzy inference system (MANFIS) with artificial bee colony (ABC) algorithm for classification of bone cancer, in: 2022 Second International Conference on Distributed Computing and High Performance Computing (DCHPC), IEEE, 2022, March, pp. 78–81.
[118] Perforated pipe improved due to nano-fluid. In Journal of Physics: Conference Series (Vol. 1973, No. 1, p. 012075). IOP Publishing.
[119] H. Al-Madhhachi, G.F. Smaisim, Experimental and numerical investigations with environmental impacts of affordable square pyramid solar still, Sol. Energy 216 (2021) 303–314.
[120] G.F. Smaisim, Investigation on heat transfer augmentation using continuous and broken ribs on a plate of heat exchanger, Int. J. Energy Environ. 9 (3) (2018).
[121] G.F. Smaisim, Augmentation of heat transfer in corrugated tube using four-start spiral wall, Al-Qadisiya J. Eng. Sci. 10 (4) (2017) 451–467.
[122] G.F. Smaisim, Enhancement heat transfer of Cu-water nanofluids with thermophysical properties modeling by artificial neural network, J. Univ. Bombay 25 (5) (2017) 1721–1735.
[123] G. Smaisim, O. Fatta, A. Valera-Medina, A. Rageb, N. Syred, Investigation of heat transfer and fluid mechanics across a heated rotating circular cylinder in crossflow, in: 54th AIAA Aerospace Sciences Meeting, 2016, p. 494.
[124] G. Smaisim, O. Fatla, A. Valera Medina, A.M. Rageb, N. Syred, Experimental and theoretical investigation of the effect of rotating circular cylinder speed on the lift and drag forces, Int. J. Energy Environ. 7 (1) (2016) 23–36.
[125] S.D. Farahani, S. Mohammadi, A.D. Farahani, G.F. Smaisim, Control of the melting process in a rectangular energy storage chamber filled with phase change material in the presence of an oscillating and rotating cylinder, J. Energy Storage 60 (2023), 106628.
[126] S. Mir, A.M. Abed, O.A. Akbari, A. Mohammadian, D. Toghraie, A. Marzban, G. F. Smaisim, Effects of curvature existence, adding of nanoparticles and changing the circular minichannel shape on behavior of two-phase laminar mixed convection of Ag/water nanofluid, Alex. Eng. J. 66 (2023) 707–730.
[127] F. Wang, N. Nasajpour-Esfahani, A.A. Alizadeh, G.F. Smaisim, A.M. Abed, S. K. Hadrawi, D. Toghraie, Thermal performance of a phase change material (PCM) microcapsules containing Au nanoparticles in a nanochannel: a molecular dynamics approach, J. Mol. Liq. (2023), 121128.
[128] Y. Chen, A.A. Alizadeh, A.M. Abed, N. Nasajpour-Esfahani, G.F. Smaisim, S. K. Hadrawi, D. Toghraie, The combustion process of methyl ester-biodiesel in the presence of different nanoparticles: a molecular dynamics approach, J. Mol. Liq. (2023), 121232.
[129] M.P. Narayanasamy, G.F. Smaisim, A.M. Abed, et al., Experimental and Computational Analysis of Pin-Fin Profiles for Aerospace Applications, Iran J Sci Technol Trans Mech Eng, 2023, https://doi.org/10.1007/s40997-022-00585-y.
[130] Y. Wang, N. Nasajpour-Esfahani, A.A. Alizadeh, G.F. Smaisim, A.M. Abed, S. K. Hadrawi, M. Hekmatifar, Numerical simulation of the melting of solid paraffin in a solar water heater and the effect of the number of fins and the height of the fins, Case Stud. Therm. Eng. 41 (2023), 102653.
[131] S.D. Farahani, S. Mohammadi, A.D. Farahani, G.F. Smaisim, Control of the melting process in a rectangular energy storage chamber filled with phase change material in the presence of an oscillating and rotating cylinder, J. Energy Storage 60 (2023), 106628.
[132] S. Mir, A.M. Abed, O.A. Akbari, A. Mohammadian, D. Toghraie, A. Marzban, G. F. Smaisim, Effects of curvature existence, adding of nanoparticles and changing the circular minichannel shape on behavior of two-phase laminar mixed convection of Ag/water nanofluid, Alex. Eng. J. 66 (2023) 707–730.
[133] A. Abderrahmane, A. Mourad, S. Mohammed, G.F. Smaisim, D. Toghraie, A. Koulali, O. Younis, Second law analysis of a 3D magnetic buoyancy-driven flow of hybrid nanofluid inside a wavy cubical cavity partially filled with porous layer and non-Newtonian layer, Ann. Nucl. Energy 181 (2023), 109511.
[134] F. Wang, N. Nasajpour-Esfahani, A.A. Alizadeh, G.F. Smaisim, A.M. Abed, S. K. Hadrawi, D. Toghraie, Thermal performance of a phase change material (PCM) microcapsules containing Au nanoparticles in a nanochannel: a molecular dynamics approach, J. Mol. Liq. (2023), 121128.
[135] Y. Chen, A.A. Alizadeh, A.M. Abed, N. Nasajpour-Esfahani, G.F. Smaisim, S. K. Hadrawi, D. Toghraie, The combustion process of methyl ester-biodiesel in the presence of different nanoparticles: a molecular dynamics approach, J. Mol. Liq. (2023), 121232.
[136] M.P. Narayanasamy, F. G, A.M. Abed, S.L. Joseph Leon, K. Subramani, Experimental and computational analysis of pin-fin profiles for aerospace applications, Iranian J. Sci. Technol., Transact. Mech. Eng. (2023) 1–11.